Virology 439 (2013) 140–151

Contents lists available at SciVerse ScienceDirect

Virology

journal homepage: www.elsevier.com/locate/yviro

Membrane association of Wuhan nodavirus protein A is required for its ability to accumulate genomic RNA1 template

Yang Qiu, Zhaowei Wang, Yongxiang Liu, Nan Qi, Meng Miao, Jie Si, Xue Xiang, Dawei Cai, Yuanyang Hu, Xi Zhou*

State Key Laboratory of Virology, College of Life Sciences, Wuhan, Hubei 430072, China

ARTICLE INFO

Article history:
Received 14 November 2012
Returned to author for revisions
16 January 2013
Accepted 13 February 2013
Available online 11 March 2013

Keywords:
Wuhan nodavirus
Protein A
Membrane association
Mitochondrial localization
Genomic RNA accumulation

ABSTRACT

One common feature of positive-strand RNA viruses is the association of viral RNA and viral RNA replicase proteins with specific intracellular membranes to form RNA replication complexes. Wuhan nodavirus (WhNV) encodes protein A, which is the sole viral RNA replicase. Here, we showed that WhNV protein A closely associates with mitochondrial outer membranes and colocalizes with viral RNA replication sites. We further identified the transmembrane domains (N-terminal aa 33-64 and aa 212-254) of protein A for membrane association and mitochondrial localization. Moreover, we found that protein A accumulates genomic RNA by stabilizing the RNA. And our further investigation revealed that the ability of WhNV protein A to associate with membranes is closely linked with its ability for membrane recruitment and stabilization of viral genomic RNA templates. This study represents an advance toward understanding the mechanism of the RNA replication of WhNV and probably other nodaviruses.

Introduction

Positive-strand (+)RNA viruses contain single-stranded RNA genomes of positive polarity, represent the largest group of viruses, and include numerous important pathogens for plants, animals, and humans (den Boon et al., 2010). One shared requirement of (+)RNA viruses is the assembly of their viral RNA replication complexes (vRCs) on host intracellular membranes (Ahlquist, 2006; Ahlquist et al., 2003; den Boon and Ahlquist, 2010; den Boon et al., 2010; Denison, 2008; Heaton and Randall, 2011; Miller and Krijnse-Locker, 2008; Nagy and Pogany, 2012; Sasvari and Nagy, 2010; Tao and Ye, 2010). For different (+)RNA viruses, vRCs form on membrane structures derived from diverse intracellular organelles, including the endoplasmic reticulum (Diaz et al., 2012; Lee et al., 2001; Mas and Beachy, 1999; Pedersen et al., 1999; Schlegel et al., 1996; Schmidt-Mende et al., 2001), Golgi apparatus (Schlegel et al., 1996), lysosomes (Froshauer et al., 1988; Kujala et al., 2001; Magliano et al., 1998; Schlegel et al., 1996), endosomes (Froshauer et al., 1988; Kujala et al., 2001) and mitochondria (Miller and Ahlquist, 2002; Miller et al., 2001). And the associations of vRCs with these distinct intracellular membranes are normally mediated by one or a few viral replication proteins carrying membrane-targeting signals, which is localized to the sites of vRCs (Ahlquist, 2006; Ahlquist et al., 2003; den Boon and Ahlquist, 2010; den Boon et al., 2010; Denison, 2008; Heaton and Randall, 2011; Miller and Krijnse-Locker, 2008; Nagy and Pogany, 2012; Sasvari and Nagy, 2010; Tao and Ye, 2010). In many cases, viral RNA replicase–intracellular membrane interactions contribute to the recruitment of viral genomic RNA template to membrane-associated sites, and this process is crucial for vRCs formation (Kopek et al., 2010; Panaviene et al., 2003; Pogany et al., 2005; Van Wynsberghe et al., 2007; Wang et al., 2005).

Nodaviruses (*Nodaviridae* family) are a family of nonenveloped positive-strand RNA viruses with $T=3$ icosahedral capsids that contain a bipartite genome of positive-sense RNAs, RNA1 and RNA2. Genomic RNA1 encodes protein A, which is the RNA-dependent RNA polymerase (RdRP) (Gallagher et al., 1983), whereas RNA2 encodes capsid precursor protein α, which undergoes autocatalytic maturation cleavage into two viral capsid proteins (Schneemann et al., 1992). Both RNA1 and RNA2 are capped but not polyadenylated (Ball and Johnson, 1999; Schneemann et al., 1998). Moreover, a subgenomic RNA3 (sgRNA3), which is not encapsidated into virion, is synthesized during RNA1 replication from the 3′ terminal of RNA1 and encodes nonstructural protein B2 that functions to suppress host RNA interference (RNAi) antiviral immunity (Cai et al., 2010; Li et al., 2002, 2005; Qi et al., 2011, 2012; Selling et al., 1990).

Nodaviral RNA replication is highly parallel with RNA replication of other (+)RNA viruses. Moreover, nodaviruses encode only

* Corresponding author. Fax: +86 27 68754941.
E-mail address: zhouxi@whu.edu.cn (X. Zhou).

0042-6822/$ - see front matter © 2013 Elsevier Inc. All rights reserved.
http://dx.doi.org/10.1016/j.virol.2013.02.010

one RNA replicase protein, RdRP (protein A), for viral RNA replication (Ahlquist, 2006; Venter and Schneemann, 2008). These features make nodaviruses such as Flock house virus (FHV) and Wuhan nodavirus (WhNV) well-recognized and simplified models for studying viral RNA replication (Castorena et al., 2010; Kampmueller and Miller, 2005; Kovalev et al., 2012; Lu et al., 2005, 2009; Qi et al., 2011, 2012; Qiu et al., 2011; Stapleford et al., 2009; Venter and Schneemann, 2008; Weeks et al., 2010). Previous studies of FHV, the most extensively studied member of the *Nodaviridae* family, revealed that protein A is localized to outer mitochondrial membranes and is a transmembrane protein with an N-terminal mitochondrial localization signal (MLS) (Miller and Ahlquist, 2002; Miller et al., 2001). Moreover, FHV protein A recruits genomic RNA templates to a membrane-associated site and multiple domains of protein A are responsible for its recruitment of RNA for vRCs formation (Kopek et al., 2010; Van Wynsberghe et al., 2007). Although FHV protein A-induced membrane association and genomic RNA accumulation have been extensively studied, the inherent correlations between these two fundamental steps of the nodaviral vRCs formation are not well understood.

As a counterpart of FHV, WhNV has been well characterized in considerable detail by our group and has been shown to be different from FHV in some aspects, such as the special strategy by which WhNV subgenomic RNA3 (sgRNA3) is synthesized (Qiu et al., 2011) and a novel RNA-binding mode of WhNV B2, an efficient viral suppressor of RNA silencing (VSR) (Qi et al., 2011, 2012). Our previous analysis of WhNV protein A sequence has predicted an N-terminal hydrophobic domain, which has the potential to associate with membranes (Liu et al., 2006). However, the assembly of WhNV vRCs in membrane-associated sites is poorly studied.

In this study, we have investigated two fundamental steps of the WhNV vRCs formation, including: (i) membrane association and organellar targeting of WhNV protein A in cells, and (ii) genomic RNA1 accumulation. We showed that WhNV protein A localizes to mitochondrial membranes, and identified two specific transmembrane domains (TMDs) which are responsible for WhNV protein A association with membranes. Moreover, WhNV protein A accumulates viral genomic RNA1 via stabilizing RNA1 and recruiting RNA1 to intracellular membranes. More importantly, our further investigation uncovered that the ability of WhNV protein A to associate with membranes is closely linked with its ability to recruit and accumulate RNA.

Results

WhNV protein A and protein A-induced RNA replication localize to mitochondria

For viral RNA replication of other nodaviruses such as FHV and Nodamura virus (NoV), protein A is the only required replicase protein, and it anchors RNA replication complexes to the outer mitochondrial membrane (Guo et al., 2004; Mezeth et al., 2007; Miller and Ahlquist, 2002; Miller et al., 2001). To determine whether this is also the case for WhNV RNA replication, we examined the subcellular localization and membrane association of WhNV protein A in Pr-E cells. This cell line is derived from *Pieris rapae* larvae, the natural host of WhNV, and was successfully utilized to study WhNV RNA replication in our previous studies (Cai et al., 2010; Qiu et al., 2011). Moreover, because WhNV RNA1 is both the template for RNA replication and the messenger for protein A synthesis, we constructed a WhNV *trans*-replication system by separating the two distinct properties of RNA1 into two separate vectors. WhNV protein A is provided by the plasmid pA (Fig. 1A), which transcribes a non-replicable protein A mRNA as previously described (Qiu et al., 2011), whereas the plasmid pAC1 is a functional template for replication, but the open reading frame (ORF) of protein A is closed by the mutation of the start codon. Thirty-six hours after transfection, the accumulation of the replication products, WhNV positive-strand (+) RNA1 and (+) sgRNA3, were examined via Northern blot analysis. The RNA replication products accumulated in cells transfected with pA plus pAC1 but not in cells transfected with pA or pAC1 alone (Fig. 1B). This WhNV *trans*-replication system was used to study viral RNA replication and the subcellular localization of protein A in the subsequent experiments.

The subcellular localization of WhNV protein A was determined via confocal immunofluorescence microscopy. WhNV protein A was expressed via transfection with plasmid pA and the mitochondria of Pr-E cells were stained with MitoTracker Red CMXRos. All experiments were repeated multiple times, and the results were digitally analyzed to examine the colocalization of protein A and mitochondria. Our results show that more than 85% protein A was localized to mitochondria. The representative results are shown in Fig. 1C. Most of WhNV protein A was localized to mitochondria in the presence or absence of the replicable RNA1 template supplied by pAC1. These results indicate that WhNV protein A localizes to mitochondria independent of other viral factors, and the *trans*-replication activity of WhNV protein A does not affect its mitochondrial localization.

After determining the mitochondrial localization of WhNV protein A, we sought to determine whether viral RNA replication also takes place in this location. To this end, viral RNA replication in cells was visualized using actinomycin D treatment and 5-bromouridine 5′-triphosphate (BrUTP) incorporation. Before and during the labeling, the cells were treated with actinomycin D to shut off the host cellular mRNA transcription from DNA. Then, the cells co-transfected with pA and pAC1 were BrUTP labeled at 36 h post-transfection for 1 h and dual labeled with anti-protein A and anti-BrUTP antibodies. Our results showed that protein A colocalized with BrUTP (Fig. 1D, top), indicating that the newly synthesized WhNV RNAs are associated with WhNV vRC. To further confirm the BrUTP signal attributed to ribonucleotide incorporation into newly synthesized RNAs but not aggregates of unincorporated BrUTP, we conducted RNase treatment, showing that the BrUTP signal was eliminated by RNase under the same condition (Fig. 1D, bottom). Taken together, these results indicate that the protein A-induced RNA replication occurs in the sites where protein A associates with the mitochondrial membrane in Pr-E cells.

Membrane association of WhNV protein A

The mitochondrial localization of protein A and viral RNA replication indicate that the RdRP and RNA template of WhNV are associated with intracellular membranes. To confirm this notion, we used equilibrium Nycodenz density gradient centrifugation to examine the flotation behavior of protein A and RNA1 from Pr-E cell lysates. The gradients were separated into six fractions and then subjected to Western or Northern blotting to detect protein A, porin, RNA1, and 18s rRNA. Protein A floated up into and was recovered in the low-density (LD) fractions (Fig. 2A, protA) that also contained the integral membrane protein porin (Fig. 2A, porin). On the other hand, although RNA1 alone was present in high-density (HD) gradient fractions (Fig. 2A, pAC1), RNA1 accumulated in the LD fractions in the presence of protein A (Fig. 2A, pA+pAC1). As previously shown (Miller and Ahlquist, 2002; Miller et al., 2001), the LD fractions represent the membrane-rich layers in the gradient, whereas the HD (non-membrane) fractions contain cytosolic soluble proteins. These results indicate that protein A and protein A-induced RNA1 replication are associated with intracellular membranes.

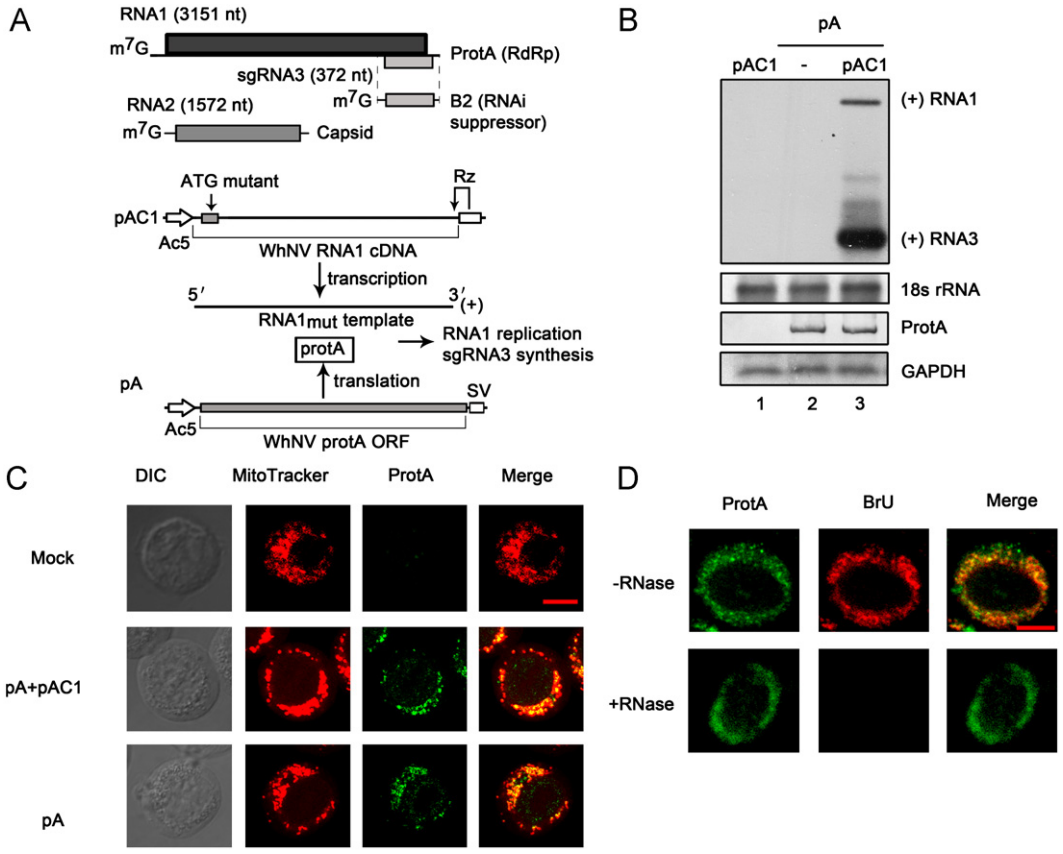

Fig. 1. WhNV protein A and protein A-induced RNA replication associate with mitochondrial membranes in Pr-E cell: (A) schematic of plasmids used for protein A (prot A) and RNA1 expression. RNA1 templates with authentic viral 5′ and 3′ termini were generated from pAC1 by precisely placing the Ac5 promoter start site and a hepatitisδribozyme (Rz), respectively, and by mutating the start codon at the indicated location to disrupt translation. The Ac5 promoter and SV40 polyadenylation signal (SV) flanking the protein A ORF in pA thereof disrupt its activity as a viral RNA replication template but maintain its RNA polymerase-directed transcription and translation. pA-derived protein A subsequently directs RNA1 replication and sgRNA3 synthesis from an RNA1 template transcribed from pAC1. (B) WhNV RNA1 replication products *in trans*-replication system. Pr-E cells were transfected with the corresponding constructs indicated above each lane. Total RNA was extracted and subjected to Northern blot analysis with probes against positive-strand (+) RNA1, (+) RNA3, and 18s rRNA. Cell lysates were also subjected to Western blot analysis using anti-protein A antibody and anti-GAPDH antibody. GAPDH, glyceraldehyde-3-phosphate dehydrogenase. (C) Localization of protein A in Pr-E cells expressing protein A. Pr-E cells were fixed at 36 h and subjected to confocal microscopy to detect the expression and localization of protein A with anti-protein A antibody (green). MitoTracker was used to distinguish the mitochondria (red). The merged image represents the digital superimposition of green and red signals, in which fluorescent areas of colocalization are yellow-orange. DIC, differential interference contrast microscopy. Scale bars, 10 μm. (D) Colocalization of protein A with nascent RNA1 in Pr-E cells transfected with pA and pAC1. At 36 h post-transfection, cells were treated with 20 μg/ml of actinomycin D for 2 h to shut off host cellular RNA polymerase. Then, 1 mM BrUTP was introduced into cells by using FuGENE HD, and cells were incubated for additional 1 h before fixation and permeabilization for dual immunofluorescent labeling as described above with anti-protein A (green) and anti-BrUTP (red) antibodies. As a specificity control, BrUTP-labeled cells were treated with RNase A at 100 μg/ml and RNase T_1 at 2 mg/ml in PBS for 30 min after cell fixation and permeabilization (bottom). The merged images represent the digital superimposition of green and red signals, in which fluorescent areas of colocalization are yellow-orange. Scale bars, 10 μm. (For interpretation of the references to color in this figure legend, the reader is referred to the web version of this article.)

Additional biochemical studies were conducted to elucidate the association between intracellular membranes and WhNV protein A. In this and subsequent experiments, the flotation gradients were divided into two fractions, LD and HD, to simplify the experimental procedures and the quantification of the flotation efficiency of protein A. The pelleted membranes and membrane-associated proteins from the lysates of Pr-E cells expressing protein A were treated with various regents as indicated for 30 min and then subjected to Nycodenz gradient fractionation (Fig. 2B). Protein A remained in the LD fraction even at pH 11.5 or in the presence of 1 M NaCl but was recovered in the HD fraction in the presence of 1.5% Triton X (TX)-100, which can dissolve membrane lipids. These results show that there is a close association between intracellular membranes and protein A.

Identification of the domains responsible for WhNV protein A membrane association

To further explore the membrane-associating properties of WhNV protein A, we sought to identify the protein A domains that mediate membrane association. We first analyzed the amino acid (aa) sequence of protein A using several programs to predict potentially hydrophobic regions that could be transmembrane domains (TMDs). Two internal regions of protein A, aa 34-59 and aa 223-244, were shown to have a high probability of being sufficiently hydrophobic and thereby being potential TMDs (Fig. 3A).

Following the computer-based prediction of TMDs, we constructed a series of protein A deletion mutants (Fig. 3B) that were then ectopically expressed in cells to assess their membrane association and subcellular localization via Nycodenz flotation analysis coupled with confocal immunofluorescence microscopy. The flotation efficiency (i.e., the proportion present in the LD fraction) of various deletion mutants ranged from 8% (Δ33-254) to 92% (Δ1-26; Fig. 3B, right row). Briefly, deleting the two predicted TMDs with or without the sequences between them (Δ33-254 or Δ33-64-212-254) efficiently blocked the membrane association of protein A (12% or 24% flotation, respectively). On the other hand, deleting either of the two predicted TMDs (Δ33-64 or Δ212-254) or deleting the sequences between the two

predicted TMDs (Δ65-212) affected the membrane association of protein A much less (65%, 72%, or 87% flotation, respectively). Moreover, the protein A mutant that destroys the RNA replicase activity of protein A by mutating its RNA replication GDD motif to GAA (protein A_{GAA}) did not affect its ability to associate with membranes (99% flotation).

The subcellular localization of the various deletion mutants was further assessed via confocal immunofluorescence microscopy using anti-protein A antibody and the mitochondrial marker Mitotracker. All the protein A mutants in which a single predicted TMD or the sequences outside the two predicted TMDs were deleted had clustered distribution and colocalized with MitoTracker (Fig. 4, Δ212-254, Δ65-211, Δ33-64, Δ255-1014), as did the full-length protein A (Fig. 4, protA). In contrast, the protein A mutants in which both of the two predicted TMDs were deleted did not colocalize with MitoTracker. Interestingly, large portions of these protein A mutants were target to nucleus (Fig. 4, Δ27-254, Δ33-254 and Δ33-64-212-254), suggesting that protein A may also contain nuclear localizing signal (NLS) like protein A from Atlantic halibut nodavirus (AHNV) (Mezeth et al., 2007). Taken together, these results elucidate the TMDs of WhNV protein A and show that the presence of either one of the two TMDs is sufficient for the mitochondrial localization of protein A.

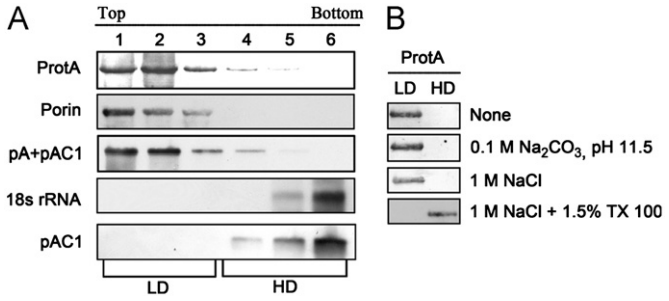

Fig. 2. Membrane association of WhNV protein A: (A) equilibrium density Nycodenz gradient fractionation of lysates from Pr-E cells expressing protein A alone or together with RNA1. Total RNA and proteins were isolated from six equal-volume fractions from each gradient and analyzed via Western blot with antibodies against protein A and Porin ("ProtA" and "Porin"), or via Northern blotting with specific probes against RNA1 and 18s rRNA ("pA+pAC1", "18s rRNA" and "pAC1"), respectively. The equal-volume fractions from the upper LD and lower HD regions were used for subsequent analysis. (B) Postnuclear lysates from Pr-E cells transfected with pA were centrifuged at 20,000*g* for 10 min; pellets were resuspended in the indicated buffer and subjected to Nycodenz gradient fractionation; and fractions were immunoblotted with anti-protein A antibody. TX-100, Triton X-100.

WhNV protein A amino acids 33–64 and 212–254 function as the mitochondrial localization signals (MLSs)

To determine whether the two TMDs (aa 33-64 and aa 212-254) of protein A could function as MLSs, we fused various protein A fragments to the N-terminal of EGFP (Fig. 5A), assessed the membrane association of the fusion proteins via Nycodenz gradient flotation, and then subjected the proteins to Western blotting with anti-EGFP antibody. EGFP alone revealed only 3% membrane association, whereas the addition of the protein A fragments containing one or both of the two TMDs, i.e. aa 33-254, aa 33-64, or aa 212-254, resulted in 77%, 69%, and 66% membrane association (flotation efficiency), respectively (Fig. 5A, right row). On the other hand, the EGFP fusion protein containing aa 65–211 (the sequences between the two TMDs) did not exhibit obvious membrane association (11% flotation) when compared to

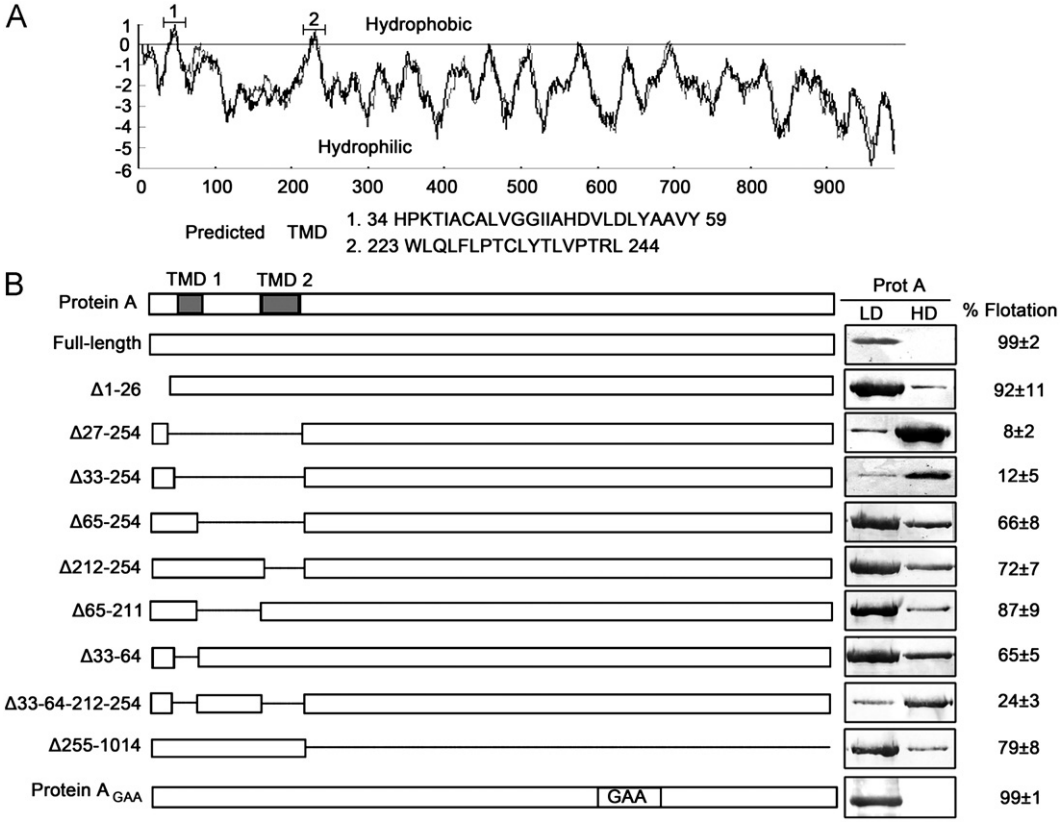

Fig. 3. WhNV protein A N-terminal aa 33-64 and 212-254 are required for membrane association: (A) potential hydrophobic regions and TMDs of protein A. The underlined amino acids represent the predicted TMDs, and the primary sequences of predicted TMDs are shown. (B) Flotation analysis was performed as described in Fig. 2 with a nested series of N-proximal deletions of protein A or with protein A deletion mutants covering aa 1-254. Flotation efficiencies represent the percentage of protein A recovered in the LD fraction compared to total protein A. S.D. values are obtained from at least three independently repeated experiments.

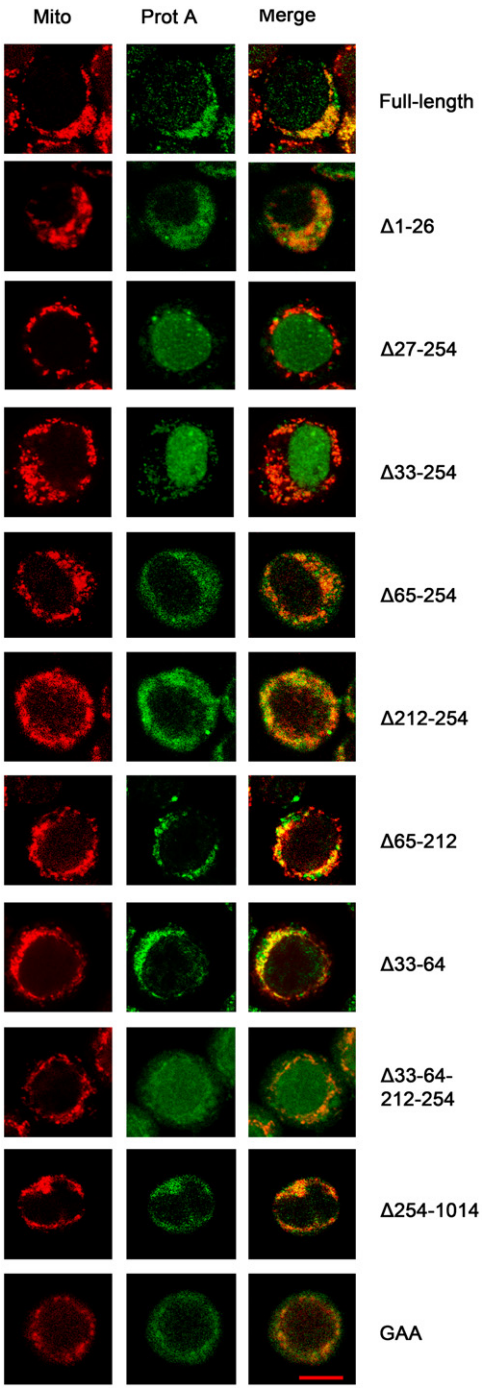

Fig. 4. Subcellular localization of WhNV protein A deletion mutants: (A) localization of protein A deletion mutants in Pr-E cells. Deletions are described in Fig. 3. Pr-E cells transfected with the indicated plasmids were immunostained with anti-protein A antibody and MitoTracker as described in Fig. 1. Scale bars, 10 μm.

EGFP alone. These results indicate that the presence of one or both of the two TMDs of WhNV protein A can mediate intracellular membrane association in cells.

We further investigated the membrane affinity of 33-64/EGFP and 212-254/EGFP under conditions designed to dislodge peripherally associated membrane proteins, similar to the experiments described for full-length protein A (Fig. 2B). Our results show that more than 50% of 33-64/EGFP and 212-254/EGFP fusion proteins remained in membrane-associated LD fractions at pH 11.5 or in the presence of 1 M NaCl but were completely recovered in the HD fraction in the presence of 1.5% Triton X (TX)-100 (Fig. 5B). Overall, these results indicate that both TMD1 (aa 33-64) and TMD2 (aa 212-254) of protein A were sufficient for the membrane insertion of protein A.

The mitochondrial membrane localization of these EGFP fusion proteins was also examined using confocal immunofluorescence microscopy (Fig. 5C). Consistent with the flotation results, the protein A fragments containing one or both of the two TMDs were distributed in a clustered fashion and colocalized with Mitotracker, whereas the EGFP fusion protein containing the sequences between the two TMDs were distributed in a similar to that of EGFP alone. These results confirmed that aa 34-64 and aa 212-254 could function as independent MLSs and further elucidated that the aa 33-64 and aa 212-254 regions are sufficient for WhNV protein A membrane association and mitochondrial localization.

Membrane association of WhNV protein A is required for RNA1 accumulation and recruitment

In many (+)RNA viruses, replicase proteins recruit viral genomic RNA to membrane sites prior to RNA replication, After determining that WhNV protein A is a mitochondrial membrane-associated protein, we sought to identify the relationship between the membrane association of protein A and protein A-mediated RNA1 accumulation.

To distinguish RNA1 from the mRNA for protein A, we inserted EGFP into the 3′ end of WhNV RNA1 (position 2929) as a reporter, resulting in the plasmid pAC1E (Fig. 6A). The replication products RNA1E and subgenomic RNA3E both contain EGFP sequences and can be detected via Northern blotting using EGFP sequence specific probes (Fig. 6B, lane 2). We also assessed the capability of the full-length and deletion mutants of WhNV protein A to support RNA1E accumulation, and Pr-E cells expressing RNA1E alone were used as a negative control (Fig. 6B–H). Moreover, protein A_{GAA} retained its RNA recruitment activity despite of losing its RNA replicase activity (Fig. 6B–H, lane 12). The RNA replication activity of most of the protein A mutants (except Δ1-26) was completely abolished (Fig. 6B and D, lanes 4–12), but the mutants still supported the accumulation of RNA1E at various levels (Fig. 6B, C, and H, lanes 4–12), indicating that protein A can accumulate RNA1E independent of RNA replication.

Multiple results showed that the ability of protein A mutants to accumulate RNA1E was closely correlated with their membrane association (Fig. 6H). Briefly, protein A Δ27–254, which had the lowest level of membrane association (8% flotation; Fig. 3B), had the least ability to accumulate RNA1E (~1.2-fold more than the negative control; Fig. 6H, lane 4), whereas protein A_{GAA}, which had complete membrane association ability (data not shown), had an ~11-fold increase in RNA1E accumulation compared with the control (Fig. 6H, lane 12). As their membrane association ability increased, the RNA1E accumulation capability of protein A mutants also gradually increased. For example, the ability of protein A Δ33–254 with 12% flotation to accumulate RNA1E was ~2.5-fold higher than that of the control (Fig. 6H, lane 5), whereas the ability of protein A Δ33-64 with 65% flotation to accumulate RNA1E was ~7-fold higher than that of the control (Fig. 6H, lane 9). On the other hand, protein A Δ255-1014, which was able to support membrane association (79% flotation), only induced a ~4-fold RNA1E accumulation (Fig. 6H, lane 11), indicating that for protein A, membrane association is required but not sufficient for the accumulation of viral genomic RNA. Taken together, these results indicate that protein A-mediated RNA1 accumulation is accompanied by the membrane association of protein A.

It is possible that some host RNA polymerases might mediate RNA1E transcription from plasmid pAC1E and thus interfere with the detection of total RNA1E accumulation. To exclude this possibility, we treated Pr-E cells with 20 μg/ml actinomycin D

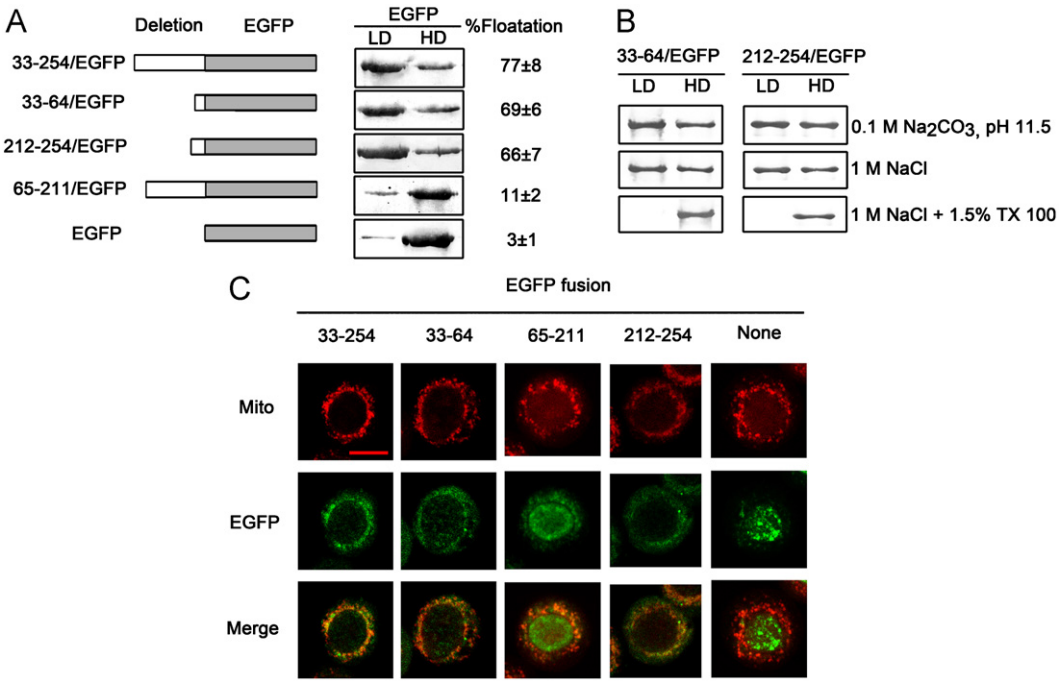

Fig. 5. N-terminal aa 33-64 and 212-254 of WhNV protein A function as the independent MLSs: (A) Pr-E cells transfected with plasmid containing the EGFP fusion constructs (left panel) were processed for Nycodenz gradient fractionation. S.D. values are obtained from at least three independently repeated experiments. (B) Pr-E cells expressing the indicated fusion proteins prepared for Nycodenz gradient fractionation as described in Fig. 2B and immunoblotted with anti-EGFP antibody. (C) Localization of EGFP fused deletion mutants of protein A in Pr-E cells. Pr-E cells transfected with the indicated plasmids were immunostained with anti-EGFP antibody and MitoTracker as described in Fig. 1. The distribution of EGFP is shown for comparison. Scale bars, 10 μm.

36 h after pAC1E transfection to inhibit cellular transcription. Cells were then harvested at six time points over the 240-min period after actinomycin D treatment, and total RNA1E was isolated and detected via Northern blotting. The half-life of RNA1E in the presence of protein A with or without RNA replicase activity (i.e., transfection with pA or pA_{GAA}) in cells was at least greater than 240 min, which is much longer than the half-life of RNA1E in the absence of protein A (~60 min; Fig. 7B). These results show that WhNV protein A efficiently stabilizes viral genomic RNA independent of its RNA replicase activity.

The ability of WhNV protein A to associate with membranes is closely related to its ability to recruit and stabilize RNA1

Although most protein A mutants were unable to replicate RNA1E (Fig. 6B), it is still possible that RNA replicase activity may affect the ability of protein A to accumulate RNA1. Therefore, to more accurately assess the correlation between protein A-mediated RNA1 accumulation and the membrane association of protein A, we chose a group of typical protein A mutants (Δ33-254, Δ33-64, Δ65-211, Δ212-254, and Δ33-64-212-254), and their RNA replication GDD motifs were all mutated to GAA. To precisely measure RNA1E accumulation, we performed real-time reverse-transcriptase polymerase chain reaction (RT-PCR) on DNase-treated RNA samples using primer sets for the EGFP and 18s rRNA sequences. Pr-E cells expressing RNA1E and protein A_{GAA} mutants were assayed to determine total RNA1E accumulation, which was graphed as the percentage of full-length protein A_{GAA}-mediated RNA1E accumulation (Fig. 8A). With the exception of some minor differences, these RT-PCR results were consistent with those described in Fig. 6H. We summarized the membrane association of protein A (Fig. 3B) and RNA1E accumulation (Fig. 6H). As shown in Fig. 8B, deletion mutants that exhibited varied reductions in protein A's membrane association displayed significant reductions in RNA1E accumulation. Thus, a correlation was observed between the disruption of membrane association ability and protein A-mediated RNA1E accumulation.

To further test the fate of RNA1E accumulated by protein A_{GAA} full-length and deletion mutants, we subjected RNA1E accumulated by protein A_{GAA} full-length and deletion mutants to Nycodenz gradient membrane flotation followed by real-time RT-PCR. In the absence of protein A_{GAA}, only a very small amount of RNA1E was present in LD fractions (~8.9% of total RNA1E), whereas in the presence of full-length protein A_{GAA}, about 90.1% of accumulated-RNA1E was recruited to the membrane-rich layer (LD fraction; Fig. 8C). Moreover, we also summarized that the capability of deletion mutants of protein A_{GAA} to recruit RNA1E to membranes was closely associated with the ability of these proteins to associate with membranes (Fig. 8D).

Using the results of these experiments, we summarize the relationships among the association of protein A with membranes, RNA1E accumulation, and the membrane association of the accumulated RNA1E as a three-dimensional (3D) graphic plots (Fig. 8E), which clearly show that as various protein A mutants gradually lose their abilities to associate with membranes, the protein A-mediated RNA1E accumulation and the membrane association of the accumulated RNA1E both correspondingly decrease. Taken together, these findings conclude that WhNV protein A accumulates viral genomic RNAs by recruiting them to intracellular membrane sites, and this process is closely coupled to the membrane association of protein A.

Discussion

The present study showed that WhNV protein A, the only RNA replicase protein required for nodaviral RNA replication is closely associated with the membranes, localizes to mitochondrial outer membranes, and colocalizes with the sites of viral RNA replication. We separated the translation and replication template functions of

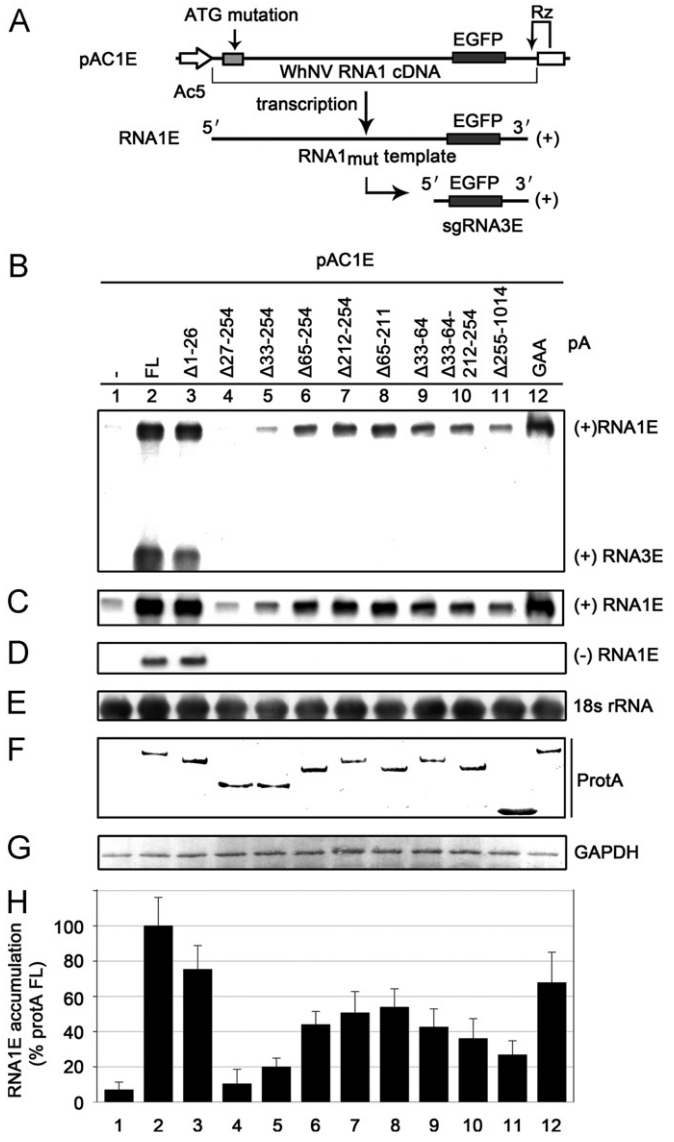

Fig. 6. Protein A induces RNA1 membrane association in Pr-E cells: (A) schematic of WhNV RNA1E and its subgenomic RNA3E. EGFP ORF was inserted in position 2929 nt of RNA1 with mutation of the start codon of protein A (pAC1E). (B–H) Pr-E cells were transfected with pAC1E alone or in combination with full-length (FL) or deletion mutants of protein A or with protein A_{GAA} (replicase defective) as indicated. Total RNA and protein were extracted and analyzed as described in Fig. 2 for (+) RNA1E and (+) RNA3E (B and C), (−) RNA1E (D), 18s rRNA (E), protein A (F), and GAPDH (G). The blots in panel C were exposed longer than those in panel B to allow for the visualization of (+) RNA1E. (H) For the indicated mutants, levels of RNA1E accumulation from at least three independent experiments after normalization to the levels of 18s rRNA were graphed as the percentage of RNA1E accumulation in the presence of full-length protein A.

WhNV RNA1 and tested the functions of protein A. We found that aa 33-64 and aa 212-254 regions are sufficient for WhNV protein A membrane association and mitochondrial localization. In association with membrane-targeting, protein A accumulates genomic RNA1. This process is induced by protein A stabilizing genomic RNA1E and recruiting RNA1E to intracellular membranes. Further investigation revealed a close correlation between the ability of protein A to associate with membranes and to recruit and accumulate genomic RNA.

The membrane association of WhNV protein A is consistent with previously identified associations between host intracellular membranes and (+)RNA virus replication (Ahlquist, 2006). Different virus groups use different intracellular membrane sites or compartments. For instance, Brome mosaic virus (BMV) takes place in the endoplasmic reticulum membranes (Wang et al., 2005), Alfalfa mosaic virus replicates at the vacuolar membrane (Van Der Heijden et al., 2001), Semliki Forest and Sindbis viruses complexes are formed at the cytoplasmic surfaces of endosomes and lysosomes (Froshauer et al., 1988), flavivirus replication happens in the trans-Golgi membranes and intermediate compartment (Mackenzie et al., 1999), and FHV replication occurs at outer mitochondrial membranes (Miller and Ahlquist, 2002; Miller et al., 2001). The precise functions of intracellular membranes in the RNA replication of (+)RNA viruses have not been fully understood, but possibly include offering an optimal microenvironment for viral RNA replicase enzymatic activities and/or facilitating the use of membrane-associated host cofactors. Our findings showed that membrane association of the WhNV protein A was resistant to extraction buffers containing a high pH, a chaotropic agent, or high ionic strength that release peripherally associated membrane proteins (Fig. 2B), indicating that protein A might be an integral membrane protein, similar to replicase proteins from some other (+)RNA viruses, such as Hepatitis C virus (Hugle et al., 2001) and poliovirus (Towner et al., 1996).

The membrane association of WhNV protein A, the colocalization of protein A and viral RNA synthesis to mitochondria provide evidence for a direct connection between nodavirus replication and mitochondrial membranes. Deletion mutants of WhNV Protein A, each containing one of the predicted TMDs (aa 33-64 and aa 212-254) localized to the mitochondria (Fig. 4). These regions also acted as MLSs independently of other WhNV Protein A region (Fig. 5). Our findings are parallel with as previous studies with other nodaviruses. Protein As from FHV, Greasy grouper nervous necrosis virus (GGNNV) and AHNV were all shown to be associated with mitochondrial outer membrane (Guo et al., 2004; Mezeth et al., 2007; Miller and Ahlquist, 2002; Miller et al., 2001). In these cases, N-terminal 46 aa of FHV protein A were sufficient for mitochondrial localization and membrane insertion (Miller and Ahlquist, 2002). MLS of GGNNV protein A is localized at N-terminal aa 215-225 (Guo et al., 2004) and AHNV protein A has two independent MLSs containing N-terminal aa 1-40 and aa 225-246 (Mezeth et al., 2007). These observations, together with our data presented here, suggest that it may be general for all members of the *Nodaviridae* family that the N-terminal region of nodaviral protein A contains the MLS.

As previously reported, protein A from AHNV also contains an NLS (Mezeth et al., 2007). Hepatitis C virus (HCV) mature core protein has an internal sequence mediating association with ER and mitochondria and also contains a bipartite NLS responsible for nuclear targeting (Suzuki et al., 2005). Moreover, FHV protein A has multiple regions responsible for membrane association (Miller and Ahlquist, 2002). The observations that large portions of WhNV protein A mutants (deleting both of the two predicted TMDs; Fig. 4, Δ27-254, Δ33-254 and Δ33-64-212-254) were localized to nucleus indicate that WhNV protein also contains NLS that is on the regions outside our identified TMD1 and TMD2, and the deletion of TMDs within WhNV protein A may make its nuclear localizing activity dominant. In addition to the TMD1 and TMD2, several additional possible transmembrane regions were predicated (aa 450-700) although they had scores below a significant threshold (Fig. 3). These transmembrane regions (aa 450-700) may also target to other cellular membranes. Alternatively, deleting TMDs may result in the conformational change of protein A and then enable protein A to target nucleus.

Although nodavirus protein A has been found to be localized to mitochondrial membranes for vRC formation, multiple evidence show that the RNA replication of (+)RNA viruses may be not limited to specific intracellular membrane (Miller et al., 2003; Xu et al., 2012). Tombusvirus replication can occur in different organellar, such as peroxisomal, ER and mitochondrial membranes

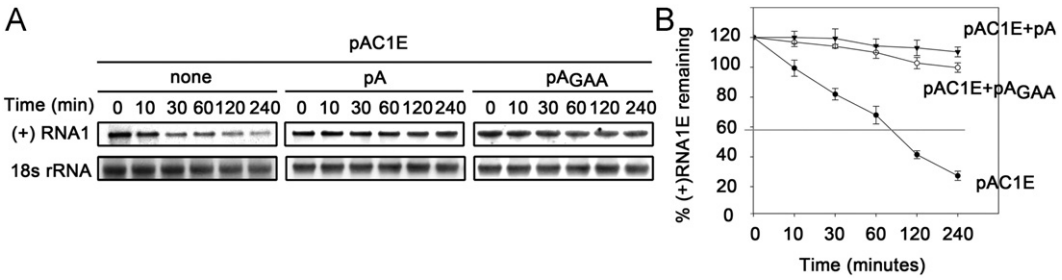

Fig. 7. Protein A stimulates RNA1 stabilization: (A) Pr-E cells transfected with pAC1E alone or in combination with pA or pA_{GAA} (protein A_{GAA}) were treated with actinomycin D 36 h after transfection. Total RNA was extracted from equal cell aliquots collected up to 240 min after treatment and analyzed via Northern blotting as described in Fig. 2. (B) RNA levels determined from three independent experiments were graphed as the percentage of (+) RNA1E remaining compared to that at the initiation of treatment.

(Xu et al., 2012). Retargeting of FHV protein A to ER support RNA replication (Miller et al., 2003). It has been previously reported by Stapleford and colleagues that FHV protein A is bound to membrane lipid and protein A interacts with several different anionic phospholipids (Stapleford et al., 2009). The affinity of FHV protein A with distinct phospholipids may help explain the robustness of FHV RNA replication in alternative intracellular membranes. Further study will be carried out to examine if this is also the case for WhNV.

In addition to associate with mitochondrial membranes, WhNV protein A induce otherwise cytoplasmic RNA1 to become membrane-associated (Fig. 2). This strong membrane localization was induced by protein A even when RNA replication activity was blocked by GAA mutation (Fig. 6). Since protein A is the only viral protein required for WhNV RNA replication and is localized to mitochondrial membranes (Figs. 1 and 2), our findings suggest that protein A recruits RNA1 prior to RNA replication to the mitochondrial membranes, where WhNV vRCs formation. These results are consistent with the previous studies on BMV, FHV and tombusviruses (Panavas et al., 2005; Panaviene et al., 2003; Pogany et al., 2005; Sharma et al., 2011; Van Wynsberghe et al., 2007; Wang et al., 2005). In these cases, BMV helicase-like protein 1a recruits BMV 2a polymerase and genomic RNAs to endoplasmic reticulum membranes to form vRCs (Wang et al., 2005) and FHV protein A recruits RNA1 to membrane-associated sites prior to RNA replication (Van Wynsberghe et al., 2007). Similarly, the p33 proteins of Tomato bushy stunt virus and Cucumber necrosis virus recruit defective interfering RNA to vRCs (Panavas et al., 2005; Panaviene et al., 2003; Pogany et al., 2005; Sharma et al., 2011).

The ability to separate the translation and replication template functions of WhNV RNA1 allowed us to investigate the inherent relationship between the membrane association of protein A and its ability to accumulate RNA1. Our deletion assays showed that the abilities of protein A mutants to accumulate RNA1, to associate with membranes and to recruit RNA1 to membrane sites were tightly coupled (Fig. 8). The accumulation of RNA1 was accomplished via stabilizing genomic RNA (Fig. 7), probably due to that the recruitment of RNA1 to membrane protected it from intracellular RNA degradation. In addition to the enhanced RNA1 stability, membrane association may also change the conformation and RNA-binding affinity of protein A. Moreover, protein A association to mitochondrial membranes would increase the local protein A concentration, probably resulting in enhanced protein A binding to RNA1. Besides, the possibility that membrane association promoted protein A association with host factors still remained.

Nodaviruses, such as FHV and WhNV, can be used as ideal models for studying the relationship between viral RNA replication and host intracellular membranes, since protein A is the only viral protein required for viral RNA replication (Ahlquist, 2006; Venter and Schneemann, 2008). The study presented here investigated two fundamental steps of the WhNV vRCs formation, include: (i) membrane association and organellar targeting of WhNV protein A; and (ii) genomic RNA accumulation. Further investigation also revealed the inherent correlation between membrane association of WhNV protein A and genomic RNA accumulation. Considering the commonalities between nodavirus and other (+)RNA viruses in RNA replication, some principles revealed here about the relationships between the membrane association of RNA replicase and genomic RNA accumulation may also apply to a range of (+)RNA viruses.

Materials and methods

Plasmids

Standard procedures were used for restriction nuclease digestion and plasmid DNA construction and purification. To analyze WhNV protein A activity in vivo, protein A ORF and RNA1 was inserted into pAC5.1/V5-His B vector (Invitrogen, Carlsbad, CA, USA). Mutations were introduced into protein A ORF via PCR-mediated mutagenesis as described previously (Qiu et al., 2011). The oligonucleotides used in this study are shown in Table 1.

Cells and transfection

Pr-E cells were maintained at 27 °C in Grace's medium (Gibco, Carlsbad, CA, USA) supplemented with 10% fetal bovine serum (Gibco). DNA plasmids were transfected into cells using FuGENE HD transfection reagent (Roche, Basel, Switzerland) according to the manufacturer's protocol. All subsequent assays were performed 36 h after transfection except where indicated otherwise.

Western blot analysis, antibodies, and fluorescent reagents

The proteins extracted from cells were subjected to 10% SDS-PAGE and Western blot analysis as previously described (Qiu et al., 2011). The rabbit anti-protein A antibody was previously described (Qiu et al., 2011). Unless otherwise indicated, all primary and secondary antibodies were purchased from Proteintech, Chicago, IL, USA. MitoTracker were purchased from Invitrogen.

Confocal immunofluorescence microscopy

Cells were incubated with 10 nM MitoTracker (Invitrogen) for 2 h. After being washed with PBS, cells were fixed with 4% paraformaldehyde in PBS for 45 min, permeabilized with 0.2% Triton X-100 for 10 min, blocked in blocking solution (PBS with 0.1% azide, 1% BSA) for 2 h, and incubated with rabbit anti-protein A antibody for 16 h and FITC-labeled goat anti-rabbit antibody for 1 h.

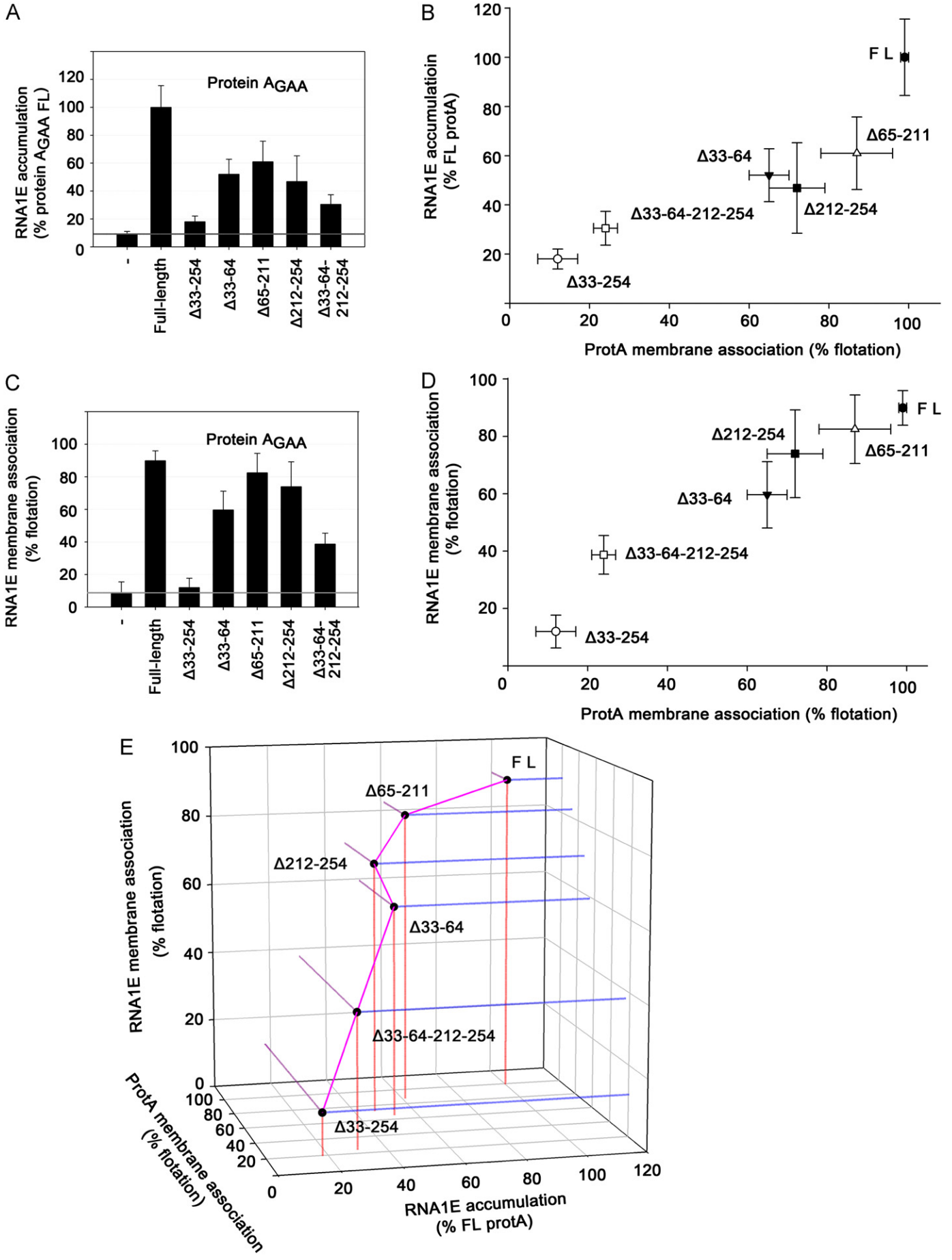
A
Protein AGAA
RNA1E accumulation (% protein AGAA FL)
120
100
80
60
40
20
0
-
Full-length
Δ33-254
Δ33-64
Δ65-211
Δ212-254
Δ33-64-212-254
B
RNA1E accumulatioin (% FL protA)
FL
Δ65-211
Δ33-64
Δ212-254
Δ33-64-212-254
Δ33-254
ProtA membrane association (% flotation)
C
Protein AGAA
RNA1E membrane association (% flotation)
D
RNA1E membrane association (% flotation)
FL
Δ212-254
Δ65-211
Δ33-64
Δ33-64-212-254
Δ33-254
ProtA membrane association (% flotation)
E
RNA1E membrane association (% flotation)
FL
Δ65-211
Δ212-254
Δ33-64
Δ33-64-212-254
Δ33-254
ProtA membrane association (% flotation)
RNA1E accumulation (% FL protA)

Table 1
Oligonucleotides used in this work.

Primers	Sequences (5′–3′)
pAC1-F	**GCGGCCGC**CTTCAAGGAATTAATTCTATATTCTAAAAAC (NotI)
pAC1-Overlap1-F	GGGCTGCGGGACCAGTTTTCATATCATAAAACGTAACGTGACAAATATAA
pAC1-Overlap1-R	TTATATTTGTCACGTTACGTTTTATGATATGAAAACTGGTCCCGCAGCCC
pAC1-Overlap2-F	TAACGTGACAAATATAAACAGCAAGACGAGTTCAGTAATCAAGACAATAGTC
pAC1-Overlap2-R	GACTATTGTCTTGATTACTGAACTCGTCTTGCTGTTTATATTTGTCACGTTA
pAC1-R	**GCGGCCGC**CTCCCTTAGCCATCCGAGTGGACGAC (NotI)
pAC1E-F	**GGCCT**ATGGTGAGCAAGGGCGA (StuI)
pAC1E-R	**GGCCT**TTACTTGTACAGCTCGTCCATGCCG (StuI)
pA_{GAA}-Overlap-F	GATAAGGTAGGGGCAGTGTTTGGTGCTGCTAGCCTAAACGCTAATCACCAAGGAG
pA_{GAA}-Overlap-R	CTCCTTGGTGATTAGCGTTTAGGCTAGCAGCACCAAACACTGCCCCTACCTTATC
pA_{GAA}-His-R1	CTAAGCGTAATCTGGAACATCGTATGGGTAGCTTAAGGAACTATTCTTAAAGACT
pA_{GAA}-His-R2	**GCGGCCGC** CTAAGCGTAATCTGGAACATCGTATGGGTAGC (NotI)
pA_{GAA}-HA-R1	CTAATGATGATGATGATGATGGCTTAAGGAACTATTCTTAAAGACTAGAG
pA_{GAA}-HA-R2	**GCGGCCGC** CTAATGATGATGATGATGATGGCTTAAGGAAC (NotI)
pA Δ1-26-F	**GGTACCCGCCACCATGGTG**CAGTATGGGTTACTACGCAGGC (KpnI)
pA Δ27-254-Overlap-F	TGCGTGTGCGTGGTGGTACGACAAGAGATAGTGTATAACGTAAC
pA Δ27-254-Overlap-R	GTTACGTTATACACTATCTCTTGTCGTACCACCACGCACACGCA
pA Δ33-254-Overlap-F	GACAACAGTATGGGTTACTACGCAGGGAGATAGTGTATAACGTAAC
pA Δ33-254-Overlap-R	GTTACGTTATACACTATCTCCCTGCGTAGTAACCCATACTGTTGTC
pA Δ65-254-Overlap-F	CAGTCTACCGGGTCGAAAATCCTTGGGAGATAGTGTATAACGTAAC
pA Δ65-254-Overlap-R	GTTACGTTATACACTATCTCCCAAGGATTTTCGACCCGGTAGACTG
pA Δ212-254-Overlap-F	CCAACAACCACGCATTAGTCTTTACTGAGATAGTGTATAACGTAACAGGTGGC
pA Δ212-254-Overlap-R	GCCACCTGTTACGTTATACACTATCTCAGTAAAGACTAATGCGTGGTTGTTGG
pA Δ65-211-Overlap-F	GCAGTCTACCGGGTCGAAAATCCTTGGACTGATGTTGACTACTATGCTAACAT
pA Δ65-211-Overlap-R	ATGTTAGCATAGTAGTCAACATCAGTCCAAGGATTTTCGACCCGGTAGACTGC
pA Δ33-64-Overlap-F	CGACAACAGTATGGGTTACTACGCAGGTGGGAATTCGTACCGACGGAGGGCC
pA Δ33-64-Overlap-R	GGGCCCTCCGTCGGTACGAATTCCCACCTGCGTAGTAACCCATACTGTTGTCG
pA Δ255-1014-R	**GCGGCCGC** GTTATTCTCAAAACGGTAAGCG (NotI)
pAC-EGFP-F	**CTCGAG**CGCCACCATGGTGAGCA AGGGCG (XhoI)
pAC-EGFP-R	**TCTAGA** TTACTTGTACAGCTCGTCCATGC (XbaI)
33-254/EGFP-F	**GGTACCCGCCACCATGGTG**CATCCTAAGACCATTGCCTGTGCACTCGTGGG (KpnI)
33-254/EGFP-R	**GCGGCCGC** GTTATTCTCAAAACGGTAAGCGAACTCATC (NotI)
33-64/EGFP-R	**GCGGCCGC** AGGATTTTCGACCCGGTAGACTGCGGC (NotI)
212-254/EGFP-F	**GGTACCCGCCACCATGGTG**CTGATGTTGACTACTATGCTAACATGAAC (KpnI)
65-211/EGFP-F	**GGTACCCGCCACCATGGTG**GAATTCGTACCGACGGAGGGCCCTAG (KpnI)
65-211/EGFP-R	**GCGGCCGC** AAAGACTAATGCGTGGTTGTTGG (NotI)
EGFP(−) probe-F	TTACTTGTACAGCTCGTCCATGCCG
EGFP(−) probe-R	TAATACGACTCACTATAGTTACTTGTACAGCTCGTCCATGCCG
EGFP(+) probe-F	ATGGTGAGCAAGGGCGAGGAGCTGTTC
EGFP(+) probe-R	GACCACTACCAGCAGAACACCCC
RT-PCR-EGFP-F	GAACTCCAGCAGGACCATGTGATC
RT-PCR-EGFP-R	AGCACCCAGTCCGCCCTGAGCA
EGFP Taqman probe	ACATCCAAGGAAGGCAGCAG
RT-PCR-18s rRNA-F	TTCGTCACTACCTCCCCGG
RT-PCR-18s rRNA-R	CGCGCAAATTACCCACTCCCGA
18s rRNA Taqman probe	CGCGCAAATTACCCACTCCCGA

Sequence specific primers are designed according to Genbank no. AY962576 (WhNV RNA1). Characters in bold indicate restriction endonuclease sites, and the types are shown in brackets. The T7 RNA polymerase promoter is shown Underlined. Kozak translation initiation sequence is indicated with bold characters in italics.

Viral RNA labeling and localization

Before RNA labeling, cells were treated with 20 μg/ml of actinomycin D (Sigma) for 2 h to shut off host cellular RNA polymerase at 36 h post-transfection. Then, 1 mM BrUTP (Sigma) was introduced into cells by using FuGENE HD (Roche) according to the manufacturer's protocol, and cells were incubated for additional 1 h before fixation and permeabilization for dual immunofluorescent labeling as described above with anti-protein A and anti-BrUTP antibodies. Immunofluorescence-labeled cells were examined via confocal scanning microscopy. For specificity control, some samples were treated with RNase A at 100 μg/ml and RNase T_1 at 2 mg/ml in PBS for 30 min after cell fixation and permeabilization but before immunostaining.

RNA extraction, northern blot analysis, and TaqMan real-time RT-PCR

Total RNA was extracted from cells using TRIzol reagent (Invitrogen) and digested with RQ1 RNase-free DNase I (Promega, Madison, WI, USA) as previously described (Qiu et al., 2011).

Fig. 8. Protein A membrane association is related to its ability to accumulate RNA1 and recruit RNA1 to a membranes: (A) Pr-E cells were transfected with pAC1E alone or in combination with the pA_{GAA} deletion mutants as described in Fig. 6. Real-time RT-PCR was performed on 5 μg of total RNA, using primers and probes specific for either RNA1E or 18s rRNA mRNA. Levels of RNA1E accumulation from four independent experiments after normalization to 18s rRNA were graphed as the percentage of RNA1E accumulation in the presence of full-length protein A_{GAA}. (B) The graph plots the RNA1E accumulation activity verses the membrane association for each of the indicated protein A_{GAA} full-length (FL) and deletion mutants. (C) Flotation and RNA extraction experiments were performed as described in Fig. 2. Levels of RNA1E accumulation from four independent experiments were graphed as the percentage of RNA1E in the LD fraction compared to that in the entire fraction (LD fraction plus HD fraction). (D) The graph plots the RNA1E membrane association activity verses the membrane association for each of the indicated protein A_{GAA} full-length (FL) and deletion mutants. (E) 3D graphic plots of the membrane association of protein A, RNA1E accumulation, and the flotation of the accumulated RNA1E in the presence of full-length protein A_{GAA} or the indicated protein A_{GAA} mutants.

For Northern blot analysis, 5 μg of each RNA sample was analyzed via Northern blot analysis as previously described (Qiu et al., 2011). The probes for positive- and negative-strand RNA1 and sgRNA3 were complementary to nt 2780-3152 of RNA1 as described previously (Qiu et al., 2011), and the probes for positive- and negative-strand EGFP were complementary to the entire EGFP sequences. All probes were labeled with DIG-UTP (Roche) for in vitro transcription; the corresponding oligonucleotides are shown in Table 1. For real-time PCR, 5 μg of RNA was subjected to reverse transcription with Superscript III reverse transcriptase (Invitrogen) using random hexamer primers (Invitrogen). The total cDNAs were then used for real-time PCR using TaqMan probes targeted for EGFP and 18s rRNA, respectively (Hoffmann et al., 2005; Huang et al., 2012; Osman et al., 2007), as shown in Table 1. PCR was carried out at 98 °C for 3 min, followed by 45 cycles at 98 °C for 15 s, 57 °C for 10 s, and 68 °C for 10 s. The identical temperature profiles were used for all real-time RT-PCR runs and fluorescence values were collected during the annealing step. All samples were analyzed in triplicate and were evaluated in at least three independent experiments.

Measurement of RNA half-life

Cell suspensions were treated with actinomycin D (Sigma) at 20 μg/ml and incubated at room temperature after 36 h transfection. Aliquots were collected before treatment and 10, 30, 60, 120 and 240 min after treatment and frozen at −70 °C before RNA extraction and subsequent analysis via Northern blotting as described above.

Membrane flotation assays

Cells were recovered via scraping and centrifugation, resuspended in hypotonic buffer, and spun at 4 °C for 15 min. Unbroken cells, nuclei, and large debris were removed via centrifugation at 500*g* for 5 min to obtain the initial total lysates. Nycodenz (Sigma) was added to the total lysates to a final concentration of 37.5% (wt/vol), and samples were loaded under a 5–25% discontinuous Nycondenz gradient prepared in hypotonic buffer and centrifuged to equilibrium at 100,000*g* for 20 h at 4 °C in a Beckman coulter SW40 rotor. After centrifugation, the gradient was divided into six equal fractions or into two fractions including the upper half of the gradient (LD fraction) and the lower half of the gradient (HD fraction). Protein samples were isolated from half of each fraction via centrifugation at 180,000*g* in a Beckman coulter SW40 rotor for 3 h and then analyzed via Western blotting. For RNA analysis, RNA was isolated from half of each fraction using TRIzol reagent as described above. Equal amounts of RNA were analyzed via Northern blotting or real-time PCR, as described above. For membrane dissociation assays, postnuclear lysates were centrifuged at 20,000*g* for 10 min to pellet membranes and their associated proteins. Pellets were resuspended in flotation buffer (0.1 M Na_2CO_3 [pH 11], 1 M NaCl, or 1 M NaCl with 1.5% Triton X-100) incubated on ice for 30 min, and fractionated in Nycodenz gradients as described above.

TMD and localization prediction

Protein sequence analysis was carried out using the following programs: DAS (Cserzo et al., 1997) (from http://www.sbc.su.se/~miklos/DAS/maindas.html), Toppred (von Heijne, 1992) (from http://mobyle.pasteur.fr/cgi-bin/portal.py?#forms::toppred), and TargerP 1.1 (Emanuelsson et al., 2000) (from http://www.cbs.dtu.dk/services/TargetP/).

Acknowledgments

We are grateful to Prof. Zehua Yu (Wuhan, China) for generously providing experimental materials. We also thank Dr. Jiali Si (Wuhan, China) for critically reading and Ms. Markeda Wade (Houston, TX, USA) for professionally editing this manuscript.

This work was supported by the National Natural Science Foundation of China Grant no. 31270190 (to X.Z.), no. 81201292 (to X.Z.) and no. 31270189 (to Y.H.), and the Chinese 111 Project Grant no. B06018.

References

Ahlquist, P., 2006. Parallels among positive-strand RNA viruses, reverse-transcribing viruses and double-stranded RNA viruses. Nat. Rev. Microbiol. 4, 371–382.
Ahlquist, P., Noueiry, A.O., Lee, W.M., Kushner, D.B., Dye, B.T., 2003. Host factors in positive-strand RNA virus genome replication. J. Virol. 77, 8181–8186.
Ball, L.A., Johnson, K.L., 1999. Reverse genetics of nodaviruses. Adv. Virus Res. 53, 229–244.
Cai, D., Qiu, Y., Qi, N., Yan, R., Lin, M., Nie, D., Zhang, J., Hu, Y., 2010. Characterization of Wuhan Nodavirus subgenomic RNA3 and the RNAi inhibition property of its encoded protein B2. Virus Res. 151, 153–161.
Castorena, K.M., Stapleford, K.A., Miller, D.J., 2010. Complementary transcriptomic, lipidomic, and targeted functional genetic analyses in cultured Drosophila cells highlight the role of glycerophospholipid metabolism in Flock House virus RNA replication. BMC Genomics 11, 183.
Cserzo, M., Wallin, E., Simon, I., von Heijne, G., Elofsson, A., 1997. Prediction of transmembrane alpha-helices in prokaryotic membrane proteins: the dense alignment surface method. Protein Eng. 10, 673–676.
den Boon, J.A., Ahlquist, P., 2010. Organelle-like membrane compartmentalization of positive-strand RNA virus replication factories. Annu. Rev. Microbiol. 64, 241–256.
den Boon, J.A., Diaz, A., Ahlquist, P., 2010. Cytoplasmic viral replication complexes. Cell Host Microbe 8, 77–85.
Denison, M.R., 2008. Seeking membranes: positive-strand RNA virus replication complexes. PLoS Biol. 6, e270.
Diaz, A., Gallei, A., Ahlquist, P., 2012. Bromovirus RNA replication compartment formation requires concerted action of 1a's self-interacting RNA capping and helicase domains. J. Virol. 86, 821–834.
Emanuelsson, O., Nielsen, H., Brunak, S., von Heijne, G., 2000. Predicting subcellular localization of proteins based on their N-terminal amino acid sequence. J. Mol. Biol. 300, 1005–1016.
Froshauer, S., Kartenbeck, J., Helenius, A., 1988. Alphavirus RNA replicase is located on the cytoplasmic surface of endosomes and lysosomes. J. Cell Biol. 107, 2075–2086.
Gallagher, T.M., Friesen, P.D., Rueckert, R.R., 1983. Autonomous replication and expression of RNA 1 from black beetle virus. J. Virol. 46, 481–489.
Guo, Y.X., Chan, S.W., Kwang, J., 2004. Membrane association of greasy grouper nervous necrosis virus protein A and characterization of its mitochondrial localization targeting signal. J. Virol. 78, 6498–6508.
Heaton, N.S., Randall, G., 2011. Multifaceted roles for lipids in viral infection. Trends Microbiol. 19, 368–375.
Hoffmann, B., Beer, M., Schelp, C., Schirrmeier, H., Depner, K., 2005. Validation of a real-time RT-PCR assay for sensitive and specific detection of classical swine fever. J. Virol. Methods 130, 36–44.
Huang, Y., Wei, H., Wang, Y., Shi, Z., Raoul, H., Yuan, Z., 2012. Rapid detection of filoviruses by real-time TaqMan polymerase chain reaction assays. Virol. Sin. 27, 273–277.
Hugle, T., Fehrmann, F., Bieck, E., Kohara, M., Krausslich, H.G., Rice, C.M., Blum, H.E., Moradpour, D., 2001. The hepatitis C virus nonstructural protein 4B is an integral endoplasmic reticulum membrane protein. Virology 284, 70–81.
Kampmueller, K.M., Miller, D.J., 2005. The cellular chaperone heat shock protein 90 facilitates Flock House virus RNA replication in Drosophila cells. J. Virol. 79, 6827–6837.
Kopek, B.G., Settles, E.W., Friesen, P.D., Ahlquist, P., 2010. Nodavirus-induced membrane rearrangement in replication complex assembly requires replicase protein a, RNA templates, and polymerase activity. J. Virol. 84, 12492–12503.
Kovalev, N., Pogany, J., Nagy, P.D., 2012. A co-opted DEAD-box RNA helicase enhances tombusvirus plus-strand synthesis. PLoS Pathog. 8, e1002537.
Kujala, P., Ikaheimonen, A., Ehsani, N., Vihinen, H., Auvinen, P., Kaariainen, L., 2001. Biogenesis of the Semliki Forest virus RNA replication complex. J. Virol. 75, 3873–3884.
Lee, W.M., Ishikawa, M., Ahlquist, P., 2001. Mutation of host delta9 fatty acid desaturase inhibits brome mosaic virus RNA replication between template recognition and RNA synthesis. J. Virol. 75, 2097–2106.
Li, H., Li, W.X., Ding, S.W., 2002. Induction and suppression of RNA silencing by an animal virus. Science 296, 1319–1321.
Liu, C., Zhang, J., Yi, F., Wang, J., Wang, X., Jiang, H., Xu, J., Hu, Y., 2006. Isolation and RNA1 nucleotide sequence determination of a new insect nodavirus from *Pieris rapae* larvae in Wuhan city, China. Virus Res. 120, 28–35.

Lu, R., Maduro, M., Li, F., Li, H.W., Broitman-Maduro, G., Li, W.X., Ding, S.W., 2005. Animal virus replication and RNAi-mediated antiviral silencing in *Caenorhabditis elegans*. Nature 436, 1040–1043.

Lu, R., Yigit, E., Li, W.X., Ding, S.W., 2009. An RIG-I-Like RNA helicase mediates antiviral RNAi downstream of viral siRNA biogenesis in *Caenorhabditis elegans*. PLoS Pathog. 5, e1000286.

Mackenzie, J.M., Jones, M.K., Westaway, E.G., 1999. Markers for trans-Golgi membranes and the intermediate compartment localize to induced membranes with distinct replication functions in flavivirus-infected cells. J. Virol. 73, 9555–9567.

Magliano, D., Marshall, J.A., Bowden, D.S., Vardaxis, N., Meanger, J., Lee, J.Y., 1998. Rubella virus replication complexes are virus-modified lysosomes. Virology 240, 57–63.

Mas, P., Beachy, R.N., 1999. Replication of tobacco mosaic virus on endoplasmic reticulum and role of the cytoskeleton and virus movement protein in intracellular distribution of viral RNA. J. Cell Biol. 147, 945–958.

Mezeth, K.B., Nylund, S., Henriksen, H., Patel, S., Nerland, A.H., Szilvay, A.M., 2007. RNA-dependent RNA polymerase from Atlantic halibut nodavirus contains two signals for localization to the mitochondria. Virus Res. 130, 43–52.

Miller, D.J., Ahlquist, P., 2002. Flock house virus RNA polymerase is a transmembrane protein with amino-terminal sequences sufficient for mitochondrial localization and membrane insertion. J. Virol. 76, 9856–9867.

Miller, D.J., Schwartz, M.D., Ahlquist, P., 2001. Flock house virus RNA replicates on outer mitochondrial membranes in Drosophila cells. J. Virol. 75, 11664–11676.

Miller, D.J., Schwartz, M.D., Dye, B.T., Ahlquist, P., 2003. Engineered retargeting of viral RNA replication complexes to an alternative intracellular membrane. J. Virol. 77, 12193–12202.

Miller, S., Krijnse-Locker, J., 2008. Modification of intracellular membrane structures for virus replication. Nat. Rev. Microbiol. 6, 363–374.

Nagy, P.D., Pogany, J., 2012. The dependence of viral RNA replication on co-opted host factors. Nat. Rev. Microbiol. 10, 137–149.

Osman, F., Leutenegger, C., Golino, D., Rowhani, A., 2007. Real-time RT-PCR (TaqMan) assays for the detection of Grapevine Leafroll associated viruses 1–5 and 9. J. Virol. Methods 141, 22–29.

Panavas, T., Hawkins, C.M., Panaviene, Z., Nagy, P.D., 2005. The role of the p33:p33/p92 interaction domain in RNA replication and intracellular localization of p33 and p92 proteins of Cucumber necrosis tombusvirus. Virology 338, 81–95.

Panaviene, Z., Baker, J.M., Nagy, P.D., 2003. The overlapping RNA-binding domains of p33 and p92 replicase proteins are essential for tombusvirus replication. Virology 308, 191–205.

Pedersen, K.W., van der Meer, Y., Roos, N., Snijder, E.J., 1999. Open reading frame 1a-encoded subunits of the arterivirus replicase induce endoplasmic reticulum-derived double-membrane vesicles which carry the viral replication complex. J. Virol. 73, 2016–2026.

Pogany, J., White, K.A., Nagy, P.D., 2005. Specific binding of tombusvirus replication protein p33 to an internal replication element in the viral RNA is essential for replication. J. Virol. 79, 4859–4869.

Qi, N., Cai, D., Qiu, Y., Xie, J., Wang, Z., Si, J., Zhang, J., Zhou, X., Hu, Y., 2011. RNA binding by a novel helical fold of b2 protein from wuhan nodavirus mediates the suppression of RNA interference and promotes b2 dimerization. J. Virol. 85, 9543–9554.

Qi, N., Zhang, L., Qiu, Y., Wang, Z., Si, J., Liu, Y., Xiang, X., Xie, J., Qin, C.F., Zhou, X., Hu, Y., 2012. Targeting of dicer-2 and RNA by a viral RNA silencing suppressor in Drosophila cells. J. Virol. 86, 5763–5773.

Qiu, Y., Cai, D., Qi, N., Wang, Z., Zhou, X., Zhang, J., Hu, Y., 2011. Internal initiation is responsible for synthesis of Wuhan nodavirus subgenomic RNA. J. Virol. 85, 4440–4451.

Sasvari, Z., Nagy, P.D., 2010. Making of viral replication organelles by remodeling interior membranes. Viruses 2, 2436–2442.

Schlegel, A., Giddings Jr., T.H., Ladinsky, M.S., Kirkegaard, K., 1996. Cellular origin and ultrastructure of membranes induced during poliovirus infection. J. Virol. 70, 6576–6588.

Schmidt-Mende, J., Bieck, E., Hugle, T., Penin, F., Rice, C.M., Blum, H.E., Moradpour, D., 2001. Determinants for membrane association of the hepatitis C virus RNA-dependent RNA polymerase. J. Biol. Chem. 276, 44052–44063.

Schneemann, A., Reddy, V., Johnson, J.E., 1998. The structure and function of nodavirus particles: a paradigm for understanding chemical biology. Adv. Virus Res. 50, 381–446.

Schneemann, A., Zhong, W., Gallagher, T.M., Rueckert, R.R., 1992. Maturation cleavage required for infectivity of a nodavirus. J. Virol. 66, 6728–6734.

Selling, B.H., Allison, R.F., Kaesberg, P., 1990. Genomic RNA of an insect virus directs synthesis of infectious virions in plants. Proc. Natl. Acad. Sci. USA 87, 434–438.

Sharma, M., Sasvari, Z., Nagy, P.D., 2011. Inhibition of phospholipid biosynthesis decreases the activity of the tombusvirus replicase and alters the subcellular localization of replication proteins. Virology 415, 141–152.

Stapleford, K.A., Rapaport, D., Miller, D.J., 2009. Mitochondrion-enriched anionic phospholipids facilitate flock house virus RNA polymerase membrane association. J. Virol. 83, 4498–4507.

Suzuki, R., Sakamoto, S., Tsutsumi, T., Rikimaru, A., Tanaka, K., Shimoike, T., Moriishi, K., Iwasaki, T., Mizumoto, K., Matsuura, Y., Miyamura, T., Suzuki, T., 2005. Molecular determinants for subcellular localization of hepatitis C virus core protein. J. Virol. 79, 1271–1281.

Tao, Y.J., Ye, Q., 2010. RNA virus replication complexes. PLoS Pathog. 6, e1000943.

Towner, J.S., Ho, T.V., Semler, B.L., 1996. Determinants of membrane association for poliovirus protein 3AB. J. Biol. Chem. 271, 26810–26818.

Van Der Heijden, M.W., Carette, J.E., Reinhoud, P.J., Haegi, A., Bol, J.F., 2001. Alfalfa mosaic virus replicase proteins P1 and P2 interact and colocalize at the vacuolar membrane. J. Virol. 75, 1879–1887.

Van Wynsberghe, P.M., Chen, H.R., Ahlquist, P., 2007. Nodavirus RNA replication protein a induces membrane association of genomic RNA. J. Virol. 81, 4633–4644.

Venter, P.A., Schneemann, A., 2008. Recent insights into the biology and biomedical applications of Flock House virus. Cell. Mol. Life Sci. 65, 2675–2687.

von Heijne, G., 1992. Membrane protein structure prediction. Hydrophobicity analysis and the positive-inside rule. J. Mol. Biol. 225, 487–494.

Wang, X., Lee, W.M., Watanabe, T., Schwartz, M., Janda, M., Ahlquist, P., 2005. Brome mosaic virus 1a nucleoside triphosphatase/helicase domain plays crucial roles in recruiting RNA replication templates. J. Virol. 79, 13747–13758.

Weeks, S.A., Shield, W.P., Sahi, C., Craig, E.A., Rospert, S., Miller, D.J., 2010. A targeted analysis of cellular chaperones reveals contrasting roles for heat shock protein 70 in flock house virus RNA replication. J. Virol. 84, 330–339.

Xu, K., Huang, T.S., Nagy, P.D., 2012. Authentic in vitro replication of two tombusviruses in isolated mitochondrial and endoplasmic reticulum membranes. J. Virol. 86, 12779–12794.